Magnetic Instruments

Invariant Calibration of Magnetic Tensor Gradiometers

Yangyi Sui[1,2], Shibin Liu[1,2], Zhijian Zhou[1,2], Yanzhang Wang[1,2], and Defu Cheng[1,2]

[1]Key Laboratory of Geo-exploration Instruments, Ministry of Education of China, Jilin University, Changchun 130026, China
[2]College of Instrumentation and Electrical Engineering, Jilin University, Changchun 130026, China

Received 22 Jan 2017, revised 16 Feb 2017, accepted 24 Feb 2017, published 2 Mar 2017, current version 7 Apr 2017.

Abstract—Magnetic tensor gradiometers are based on multiple sensors arranged in a unified coordinate system. Current calibration methods focus on each gradient tensor component separately, rather than the entire tensor system, so the advantages of tensor measurement are not completely realized. In this letter, the nonorthogonal error, misalignment error, scale-factor error, and zero offset in a magnetic tensor gradiometer with multiple elements are modeled. Optimal correction parameters are obtained by using two independent rotation invariants of the magnetic gradient tensor.

Index Terms—Magnetic instruments, calibrations, magnetic tensor gradiometers.

I. INTRODUCTION

Magnetic tensor gradiometers measure the gradients of three orthogonal magnetic field components [Pedersen 1990]. They are used in scientific research and production, especially in the Earth's magnetic field, where the magnetic gradient tensor is derived from the vector field. Magnetic tensor gradiometers have been used in many applications, such as buried object detection [Pei 2010], magnetic dipole localization [Nara 2006], remote determination of magnetic properties [Clark 1998], monitoring the Kilauea volcano [Bracken 1998], study of global magnetic models [Schiffler 2014a], detection of magnetic nanoparticles [Elrefai 2015], characterization of magnetic disturbances [Griffin 2012], and evaluation of magnetically shielded rooms [Voigt 2015].

There are three types of magnetic gradient tensors according to different measurement principles, namely, first-order Taylor series expansion [Schmidt 2004, Stolz 2006, Sui 2014], rotating modulation [Tilbrook 2009], and string vibration [Sunderland 2009]. No matter what measurement principle it takes, the calibration of a magnetic tensor gradiometer is indispensable. Because of the ubiquity of the Earth's magnetic field, it is natural to use it to obtain the calibration parameters. If a so-called gradiometer imbalance exists, the output of the tensor gradiometer in a uniform field should be a function of the Earth's magnetic field [Schiffler 2014b]. Therefore, if the gradient tensor components and the magnetic fields can be measured simultaneously when rotating the tensor gradiometer in a uniform field, the calibration parameters can be obtained by using the least squares [Pang 2014, Yin 2015] or the linearly constrained least-squares-fit [Keene 2005].

There are still two problems in this method. One is that zero being the output of a single tensor component in a uniform magnetic field is a necessary but not a sufficient condition for the correction of the tensor gradiometer. It cannot ensure the correctness of the construction of multiple gradient components. In particular, for those tensor gradiometers that can measure gradients directly, this method still remains at the correction stage of the gradient imbalance of the sensors. The other problem with this method is that the reference vector magnetometer also requires precise calibration due to the scale-factor, nonorthogonal, misalignment, zero-offset errors [Schiffler 2014]. Typical vector magnetometer calibration methods require an accurate magnitude of reference of the magnetic field [Merayo 2000, Gemoz-Egziabher 2006]. Not only is the correction procedure complicated, but the performance of the tensor gradiometer is restricted by the auxiliary magnetometers.

The complete calibration of the magnetic tensor gradiometer actually consists of two levels. The first one is the calibration of each gradient tensor component. The second one is the calibration of the construction of multiple gradient components. It is difficult to uniformly express the error mechanisms of gradient components obtained by different measurement principles, but the errors are similar when constructing the tensor gradiometer. Therefore, the work in this letter focuses on the second level. First, the models are built for the nonorthogonal error, misalignment, scale-factor error, and zero offset in the construction of a magnetic tensor gradiometer by composing multiple elemental gradiometers. Then, the optimal correction parameters are obtained by using the two independent rotation invariants of the magnetic gradient tensor.

II. ERROR MODEL OF TENSOR GRADIOMETER

Let $\boldsymbol{B}$ be the magnetic induction vector with three components B_x, B_y, and B_z. The magnetic gradient tensor $\boldsymbol{G}$ is comprised of the gradients of the three field components. Potential field theory stipulates that the gradient tensor is symmetric and traceless, so $\boldsymbol{G}$ only has five independent components [Pedersen 1990] and can be expressed by

$$\boldsymbol{G}=\begin{bmatrix}\frac{\partial B_x}{\partial x} & \frac{\partial B_x}{\partial y} & \frac{\partial B_x}{\partial z}\\ \frac{\partial B_y}{\partial x} & \frac{\partial B_y}{\partial y} & \frac{\partial B_y}{\partial z}\\ \frac{\partial B_z}{\partial x} & \frac{\partial B_z}{\partial y} & \frac{\partial B_z}{\partial z}\end{bmatrix}=\begin{bmatrix}G_{xx} & G_{xy} & G_{xz}\\ G_{xy} & G_{yy} & G_{yz}\\ G_{xz} & G_{yz} & -G_{xx}-G_{yy}\end{bmatrix}. \tag{1}$$

Corresponding author: Y. Sui (e-mail: suiyangyi@jlu.edu.cn).
Digital Object Identifier 10.1109/LMAG.2017.2677381

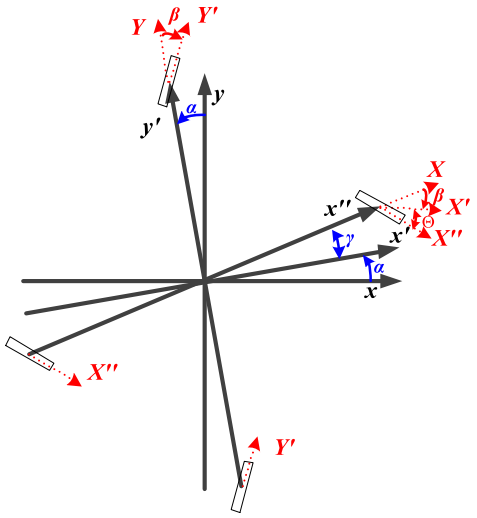

Fig. 1. Two-dimensional schematic of the installed elemental gradiometer with the nonorthogonal angle γ between the x''-axis and the y'-axis, and the other nonorthogonal angle θ between the sense direction of X'' and Y', apart from the misalignment angle α and β in the baseline and the sense direction. The dotted and solid arrows indicate the sense directions and the baseline directions of the gradiometers, respectively.

A. Misalignment and Nonorthogonal Error in Two-Dimensional Space

There are misalignments and nonorthogonal errors in the manufacturing and installation process. Fig. 1 shows two installed elemental gradiometers with the misalignment angles α and β in the baseline and sense direction, respectively. The sense direction of Y' is equivalent to the sense direction of Y being rotated twice with respect to angles α and β.

As well as the misalignment angles, the installed elemental gradiometer with the nonorthogonal angle γ between the x''-axis and the y'-axis and the other nonorthogonal angle θ between the sense direction of X'' and Y' is also shown in Fig. 1. The actual gradient of g_{xx} is the change of the magnetic field component X'' in the x''-axis direction.

The desired tensor in the two-dimensional (2-D) space is

$$\boldsymbol{G} = \begin{bmatrix} G_{xx} & G_{xy} \\ G_{yx} & G_{yy} \end{bmatrix}. \tag{2}$$

Therefore, if the actual measured gradient component G_{yy} has errors, as shown in Fig. 1, that is the sense direction of Y' is equivalent to the sense direction of Y being rotated twice with angles α and β, and the baseline direction has been rotated with angle α. Misalignments can be treated as the rotational transformations of coordinates which are similarly given in Pedersen [1990].

Besides the misalignment in the measured G_{yy}, the measured gradient component G_{xx} has the nonorthogonal angle γ in the baseline. The sense direction has been rotated with angle γ because of the nonorthogonal error in the baseline. In addition, there exists another nonorthogonal angle θ between the sense directions of X'' and Y'. Assume that R_{xx} is the measured G_{xx}, which can be calculated using (3), and N_{x11} in $\boldsymbol{N}_x$ is R_{xx}:

$$\begin{aligned} N_{\boldsymbol{x}} = \begin{bmatrix} N_{x11} & N_{x12} \\ N_{x21} & N_{x22} \end{bmatrix} &= \begin{bmatrix} c_\theta & s_\theta \\ 0 & 1 \end{bmatrix} \\ &\times \begin{bmatrix} c_\gamma & s_\gamma \\ -s_\gamma & c_\gamma \end{bmatrix} \begin{bmatrix} c_\beta & s_\beta \\ -s_\beta & c_\beta \end{bmatrix} \begin{bmatrix} c_\alpha & s_\alpha \\ -s_\alpha & c_\alpha \end{bmatrix} \\ &\times \begin{bmatrix} G_{xx} & G_{xy} \\ G_{yx} & G_{yy} \end{bmatrix} \begin{bmatrix} c_\alpha & s_\alpha \\ -s_\alpha & c_\alpha \end{bmatrix}^{\mathrm{T}} \begin{bmatrix} c_\gamma & s_\gamma \\ 0 & 1 \end{bmatrix}^{\mathrm{T}} \end{aligned} \tag{3}$$

where s_* and c_* denote sine and cosine function.

The other error models of the tensor gradiometer in the 2-D space can also be defined in an analogous manner.

B. Misalignment and Nonorthogonal Error in Three-Dimensional Space

We take tensor components G_{xx} and G_{yy} as examples to derive the error models in three-dimensional (3-D) space.

1) If there are three misalignment angles α_1, β_1, and γ_1 in the baseline directions, the elemental gradiometers can be treated as being rotated about three axes and the transformation matrix is expressed by $\boldsymbol{M}$. If there are three misalignment angles α_2, β_2, and γ_2 in the sense directions, the transformation matrix is defined by $\boldsymbol{L}$ likewise.
2) If there are three nonorthogonal angles α_3, β_3, and γ_3 in the baseline directions, the new axes are x', y', and z. That is, the actual z-axis and the ideal z-axis are coaxial and the $y'oz$ plane and the yoz plane are coplanar; δ_3 is the angle between the y'-axis and y-axis; p is the projection from the x'-axis onto the xoy plane and α_3 is the angle between the x'-axis and p; β_3 is the angle between the x-axis and p, so the nonorthogonal matrix is defined by $\boldsymbol{W}_3$. The sense directions are also affected by the nonorthogonal errors of the baseline simultaneously. The sense direction of X' is equivalent to the sense direction of X being rotated twice with angles β_3 and α_3 about the z-axis and the y-axis, respectively, and the transformation matrix is defined by $\boldsymbol{W}_2$. The sense direction of Y' is equivalent to the sense direction of Y being rotated with angle δ_3 about the x-axis and the transformation matrix is defined by $\boldsymbol{W}_5$.
3) If there are three nonorthogonal angles α_4, β_4, and γ_4 in the sense directions, the nonorthogonal matrix and transformation matrix can be derived in an analogous manner and expressed by $\boldsymbol{W}_1$ and $\boldsymbol{W}_4$.

Assume that R_{xx} and R_{yy} are the measured G_{xx} and G_{yy}, which can be calculated via (4) and (5). N_{x11} and N_{y22} in $\boldsymbol{N}_x$ and $\boldsymbol{N}_y$ are R_{xx} and R_{yy}, respectively.

$$N_{\boldsymbol{x}} = \begin{bmatrix} N_{x11} & N_{x12} & N_{x13} \\ N_{x21} & N_{x22} & N_{x23} \\ N_{x31} & N_{x32} & N_{x33} \end{bmatrix} = W_1 L W_2 M G M^{\mathrm{T}} W_3^{\mathrm{T}} \tag{4}$$

$$N_{\boldsymbol{y}} = \begin{bmatrix} N_{y11} & N_{y12} & N_{y13} \\ N_{y21} & N_{y22} & N_{y23} \\ N_{y31} & N_{y32} & N_{y33} \end{bmatrix} = W_4 L W_5 M G M^{\mathrm{T}} W_3^{\mathrm{T}} \tag{5}$$

where

$$M = \begin{bmatrix} c_{\beta_1}c_{\alpha_1} & s_{\alpha_1}c_{\beta_1} & -s_{\beta_1} \\ s_{\gamma_1}s_{\beta_1}c_{\alpha_1} - c_{\gamma_1}s_{\alpha_1} & s_{\gamma_1}s_{\beta_1}s_{\alpha_1} - c_{\gamma_1}c_{\alpha_1} & s_{\gamma_1}c_{\beta_1} \\ c_{\gamma_1}s_{\beta_1}c_{\alpha_1} + s_{\gamma_1}s_{\alpha_1} & c_{\gamma_1}s_{\beta_1}s_{\alpha_1} - s_{\gamma_1}c_{\alpha_1} & c_{\gamma_1}c_{\beta_1} \end{bmatrix},$$

$$L = \begin{bmatrix} c_{\beta_2}c_{\alpha_2} & s_{\alpha_2}c_{\beta_2} & -s_{\beta_2} \\ s_{\gamma_2}s_{\beta_2}c_{\alpha_2} - c_{\gamma_2}s_{\alpha_2} & s_{\gamma_2}s_{\beta_2}s_{\alpha_2} - c_{\gamma_2}c_{\alpha_2} & s_{\gamma_2}c_{\beta_2} \\ c_{\gamma_2}s_{\beta_2}c_{\alpha_2} + s_{\gamma_2}s_{\alpha_2} & c_{\gamma_2}s_{\beta_2}s_{\alpha_2} - s_{\gamma_2}c_{\alpha_2} & c_{\gamma_2}c_{\beta_2} \end{bmatrix},$$

$$W_1 = \begin{bmatrix} c_{\beta_4}c_{\alpha_4} & s_{\beta_4}c_{\alpha_4} & s_{\alpha_4} \\ 0 & 1 & 0 \\ 0 & 0 & 1 \end{bmatrix}, W_2 = \begin{bmatrix} c_{\beta_3}c_{\alpha_3} & c_{\alpha_3}s_{\beta_3} & -s_{\alpha_3} \\ 0 & 1 & 0 \\ 0 & 0 & 1 \end{bmatrix},$$

$$W_3 = \begin{bmatrix} c_{\beta_3}c_{\alpha_3} & s_{\beta_3}c_{\alpha_3} & s_{\alpha_3} \\ 0 & c_{\delta_3} & s_{\delta_3} \\ 0 & 0 & 1 \end{bmatrix}, W_4 = \begin{bmatrix} 1 & 0 & 0 \\ 0 & c_{\delta_4} & s_{\delta_4} \\ 0 & 0 & 1 \end{bmatrix}$$

$$W_5 = \begin{bmatrix} 1 & 0 & 0 \\ 0 & c_{\delta_3} & s_{\delta_3} \\ 0 & 0 & 1 \end{bmatrix}.$$

Therefore, the measured component $R_{\mu\upsilon}$ (μ, $\upsilon = x$, y, and z) only contains the misalignment and nonorthogonal error, which can be expressed by

$$R_{\mu\upsilon} = \sum_{i,j=x,y,z} p_{ij} G_{ij}. \tag{6}$$

C. Error Model of the Magnetic Tensor Gradiometer

The actual measured tensor component $T_{\mu\upsilon}$ also has the scale-factor error c, and zero offset o, and is expressed by

$$T_{\mu\upsilon} = c_{\mu\upsilon} N_{\mu\upsilon} + o_{\mu\upsilon}. \tag{7}$$

Therefore, the error model of five independent tensor components can be expressed by

$$T = K\hat{G} + O \tag{8}$$

where $\hat{G} = (G_{xx}, G_{xy}, G_{xz}, G_{yy}, G_{yz})^T$.

The correction model of the tensor component can be rewritten as

$$\hat{G} = K^{-1}T - K^{-1}O = HT + D. \tag{9}$$

There are 30 coefficients, including 25 in $\boldsymbol{H}$, denoted as h_{ij}, and five in $\boldsymbol{D}$ denoted as d_{ij}.

III. CALIBRATION METHOD OF THE TENSOR GRADIOMETER

An invariant is a constant by a particular transformation of coordinates. There are two nonzero invariants given by Pedersen:

$$I_1 = -\frac{1}{2} \sum_{\mu,\upsilon=x,y,z} G_{\mu\upsilon}^2 \tag{10}$$

$$I_2 = |G|. \tag{11}$$

A. Using the Invariant I_1

The first step is using invariant I_1, that is, (12) can be obtained by substituting $G_{\mu\upsilon}$ in (10) by the five independent tensor measurements $T_{\mu\upsilon}$ in (9).

$$F(x_1, x_2, \ldots, x_{20}) = x_1 T_{xx}^2 + x_2 T_{xy}^2 + x_3 T_{xz}^2 + x_4 T_{yy}^2 + x_5 T_{yz}^2 + 2x_6 T_{xx} T_{xy} + \ldots + 2x_{20} T_{yz} = 1 \tag{12}$$

where $x_1 - x_{15}$ are quadratic polynomials of h_{ij}, and $x_{16} - x_{20}$ are the combinations of polynomials of h_{ij} and d_{ij}.

When the magnetic tensor gradiometer is rotated around its center, it can measure n sets of tensors with errors. According to the invariant property $x_1 - x_{20}$ should keep F_i ($i = 1 \ldots n$) constant. Accordingly, we design the function J in (13) and calculate the optimal $x_1 - x_{20}$ using the least squares method:

$$J(x_1, x_2, x_3, \ldots, x_{20}) = \min \left(\sum_{i=1}^{n} [F_i(x_1, x_2, x_3, \ldots, x_{20}) - 1]^2 \right). \tag{13}$$

The combination of (9), (10), and (12) can be expressed as

$$(T - O)^{\mathrm{T}} A (T - O) = 1 \tag{14}$$

where

$$A = \begin{bmatrix} x_1 & x_6 & x_7 & x_8 & x_9 \\ x_6 & x_2 & x_{10} & x_{11} & x_{12} \\ x_7 & x_{10} & x_3 & x_{13} & x_{14} \\ x_8 & x_{11} & x_{13} & x_4 & x_{15} \\ x_9 & x_{12} & x_{14} & x_{15} & x_5 \end{bmatrix}, \; O = -A^{-1} \begin{bmatrix} x_{16} \\ x_{17} \\ x_{18} \\ x_{19} \\ x_{20} \end{bmatrix}.$$

So the zero offset $\boldsymbol{O}$ can be obtained by coefficients $x_1 - x_{20}$. After removing the zero offset, (9) and (12) can be expressed as

$$\begin{cases} T' = T - O = K\hat{G} \\ \hat{G} = HT' \end{cases} \tag{15}$$

$$F(y_1, y_2, \ldots, y_{15}) = y_1 T_{xx}'^2 + y_2 T_{xy}'^2 + y_3 T_{xz}'^2 + y_4 T_{yy}'^2 + y_5 T_{yz}'^2 + \cdots + 2y_{15} T'_{yy} T'_{yz} = I_1. \tag{16}$$

Likewise, $y_1 - y_{15}$ are quadratic polynomials of h_{ij} and can be calculated by the least squares method.

We take the example of the coefficient y_1:

$$y_1 = 2h_{11}^2 + 2h_{11}h_{31} + h_{21}^2 + h_{31}^2 + 2h_{41}^2 + 2h_{51}^2. \tag{17}$$

Accordingly, 15 equations denoted as E_1 can be obtained. Since the number of equations is less than the number of unknowns, the invariant I_2 needs to be used.

B. Using the Invariant I_2

By expanding (11), we obtain a cubic polynomial of $G_{\mu\upsilon}$

$$I_2 = -G_{xx}^2 G_{yy} + G_{xx} G_{xy}^2 - G_{xx} G_{yy}^2 - G_{xx} G_{yz}^2 + G_{xy}^2 G_{yy} + 2G_{xy} G_{xz} G_{yz} - G_{xz}^2 G_{yy}. \tag{18}$$

Equation (19) can be obtained by substituting $\hat{G}$ in (18) by the $\boldsymbol{T}'$ in (15):

$$N(z_1, z_2, \ldots, z_{35}) = z_1 T_{xx}'^3 + z_2 T_{xx}'^2 T'_{xy} + z_3 T'_{xx} T'^2_{xz} + z_4 T_{xx}'^2 T'_{yy} + z_5 T'_{xx} T'^2_{yz} + z_6 T'_{xx} T'_{xy} T'_{xz} + \cdots + z_{35} T_{yz}'^3 = I_2 \tag{19}$$

TABLE 1. Error coefficients in simulation.

Scale-factor error	Uniform distribution with amplitude of 0.01
Nonorthogonal errors	Uniform distribution with amplitude of 1°
Misalignments	Uniform distribution with amplitude of 3°
Zero offsets	Uniform distribution with amplitude of 15 nT/m
Magnetic gradient noise	Uniform distribution with amplitude of 0.1 nT/m

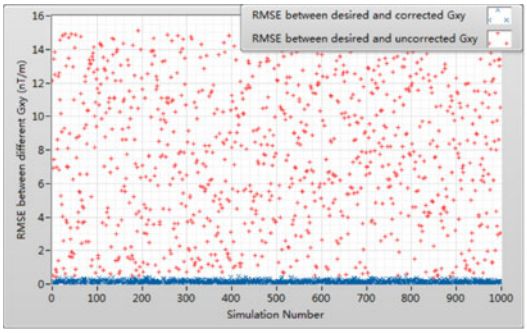

Fig. 2. RMSE between the desired and the uncorrected G_{xy} (red plus sign markers) and the corrected G_{xy} (blue cross markers) in the 1000 simulations.

where $z_1 - z_{35}$ are cubic polynomials of h_{ij} and can be calculated by the least-squares method likewise.

Accordingly, 35 equations denoted as E_2 can be obtained. That is, we have 50 equations and 25 unknowns and can get the numerical solution with MATLAB. Eventually, the calibrated tensor can be obtained through (9).

IV. SIMULATION EXPERIMENTS

A. Performance Assessment

There are five installed gradiometers measuring five independent components G_{xx}, G_{xy}, G_{xz}, G_{yy}, and G_{yz} in simulation experiments. The procedure of simulation is as follows.

1) The true value of the magnetic gradient tensor formed by the magnetic dipole, whose magnetic moment vector is (250 000, 250 000, −353 553.39) A · m^2 is calculated through the equation in Sui [2015].
2) The measured magnetic gradient tensors are calculated by the true value, error coefficients, and random rotation angles. Error coefficients are shown in Table 1.
3) The calibration coefficients are obtained by the proposed method and applied to correct the measured magnetic gradient tensors.

The simulation is repeated 1000 times and all coefficients are generated according to Table 1. The root mean square error (RMSE) is used to evaluate the error between the desired and the uncorrected G_{xy}, and the corrected G_{xy}, respectively. The results of a pair of RMSEs in each simulation are shown in Fig. 2. The average RMSE is reduced from 7.50 to 0.13 nT/m after correction. The results of other components are similar to G_{xy} and shown in Table 2. The improvement ratios range from 38.58 to 60.83.

B. Simulation of a Survey Line

The magnetic dipole is used as the target at a depth of 5 m under the ground. A 100 m survey line containing 500 observation points is designed right above the target at a height of 10 m. Fig. 3 shows the result of the comparison among the desired, corrected, and uncorrected tensor magnitudes, C_T, on the survey line. The RMSE is reduced from 17.73 to 0.11 nT/m after the correction. The results of five components are similar to C_T and shown in Table 3. The improvement ratios range from 30.15 to 99.89.

TABLE 2. Average RMSEs of five tensor components in the 1000 simulations.

	G_{xx}	G_{xy}	G_{xz}	G_{yy}	G_{yz}
Before correction (nT/m)	7.30	7.50	7.50	7.33	7.54
After correction (nT/m)	0.12	0.13	0.18	0.19	0.15
Improvement ratio	60.83	57.70	41.67	38.58	50.27

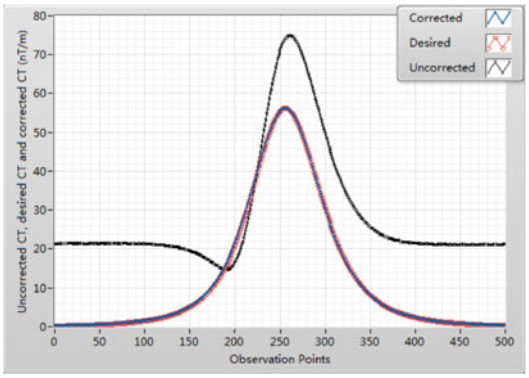

Fig. 3. The desired (red line with circle markers), corrected (blue line with point markers), and uncorrected C_T (black line with cross markers) in the survey line.

TABLE 3. RMSEs of five tensor components in one simulation.

	G_{xx}	G_{xy}	G_{xz}	G_{yy}	G_{yz}
Before correction (nT/m)	5.00	3.92	9.77	6.98	8.99
After correction (nT/m)	0.08	0.13	0.25	0.14	0.09
Improvement ratio	62.50	30.15	39.08	49.86	99.89

V. CONCLUSION

The calibration method for the magnetic tensor gradiometer is one of the most decisive factors for its application. In this letter, a calibration method has been proposed using two tensor invariants as constraints, which is similar to the scalar calibration of vector magnetometers. The derived calibration parameters ensure the best overall performance. Starting from specific sensors, the method can be generalized to error models for other magnetic tensor gradiometers.

ACKNOWLEDGMENT

This work was supported by the National Natural Science Foundation of China under Grant 41574174.

REFERENCES

Bracken R E, Grover T P, Puniwai G S (1998), "Development and testing of a tensor magnetic gradiometer system with trial monitoring near the Kilauea Volcano, Hawaii," U.S. Dept. of the Interior, U.S. Geological Survey, Tech. Rep. no. 98-773, [Online]. Available: https://pubs.er.usgs.gov/publication/ofr98773

Clark D A, Schmidt P W, Coward D A, Huddleston M P (1998), "Remote determination of magnetic properties and improved drill targeting of magnetic anomaly sources by Differential Vector Magnetometry (DVM)," *Explor. Geophys.*, vol. 29, pp. 312–319, doi: 10.1071/EG998312.

Elrefai A L, Sasada I, Yoshida T (2015), "Fluxgate gradiometer for magnetic nanoparticle magnetorelaxometry in unshielded environment," in *Proc. IEEE Int. Magn. Conf.*, Beijing, China, CT-09, doi: 10.1109/INTMAG.2015.7156945.

Gemoz-Egziabher D, Elkaim G H, Powell D, Parkinson B W (2006), "Calibration of strapdown magnetometers in magnetic field domain," *J. Aerosp. Eng.*, vol. 19, pp. 87–102, doi: 10.1061/(ASCE)0893-1321(2006)19:2(87).

Griffin D K, Masseglia O, Hall M, Trougnou L, Hewitson M, Howe C, Poyntz-Wright O, Leopoldi M, Ding L, Turner S, Harmon S (2012), "Design and calibration of a compact low-noise magnetic gradiometer," in *Proc. ESA Workshop Aerosp. EMC*, Venice, Italy, pp. 1–6, [Online]. Available: http://ieeexplore.ieee.org/document/6232577/

Keene M N, Humphrey K P, Horton T J (2005), "Actively shielded, adaptively balanced SQUID gradiometer system for operation aboard moving platforms," *IEEE Trans. Appl. Supercond.*, vol. 15, pp. 761–764, doi: 10.1109/TASC.2005.850046.

Merayo J M G, Brauer P, Primdahl F, Petersen J R, Nielsen O V (2000), "Scalar calibration of vector magnetometers," *Meas. Sci. Technol.*, vol. 11, pp. 120–132, doi: 10.1088/0957-0233/11/2/304.

Nara T, Suzuki S, Ando S (2006), "A closed-form formula for magnetic dipole localization by measurement of its magnetic field and spatial gradients," *IEEE Trans. Magn.*, vol. 42, pp. 3291–3293, doi: 10.1109/TMAG.2006.879151.

Pang H, Pan M, Wan C, Chen J, Zhu X, Luo F (2014), "Integrated compensation of magnetometer array magnetic distortion field and improvement of magnetic object localization," *IEEE Trans. Geosci. Remote Sens.*, vol. 52, pp. 5670–5676, doi: 10.1109/TGRS.2013.2291839.

Pedersen L B, Rasmussen T M (1990), "The gradient tensor of potential field anomalies: Some implications on data collection and data processing of maps," *Geophysics*, vol. 55, pp. 1558–1566, doi: 10.1190/1.1442807.

Pei Y H, Yeo H G, Kang X Y, Pua S L, Tan J (2010), "Magnetic gradiometer on an AUV for buried object detection," in *Proc. MTS/IEEE Oceans*, Seattle, WA, USA, pp. 1–8, doi: 10.1109/OCEANS.2010.5664272.

Schiffler M, Queitsch M, Schneider M, Goepel A, Stolz R, Krech W, Meyer H-G, Kukowski N (2014a), "Calculation and analysis of magnetic gradient tensor components of global magnetic models," in *Proc. Amer. Geophys. Union Fall Meeting Abstr.*, San Francisco, CA, USA, vol. 1, [Online]. Available: http://meetingorganizer.copernicus.org/EGU2014/EGU2014-9080.pdf

Schiffler M, Queitsch M, Stolz R, Chwala A, Krech W, Meyer H-G, Kukowski N (2014b), "Calibration of SQUID vector magnetometers in full tensor gradiometry systems," *Geophys. J. Int.*, vol. 198, pp. 954–964, doi: 10.1093/gji/ggu173.

Schmidt P, Clark D, Leslie K, Bick M, Tilbrook D, Foley C (2004), "GETMAG–A SQUID magnetic tensor gradiometer for mineral and oil exploration," *Explor. Geophys.*, vol. 35, pp. 297–305, doi: 10.1071/EG04297.

Stolz R, Zakosarenko V, Schulz M, Chwala A, Fritzsch L, Meyer H-G, Köstlin E O (2006), "Magnetic full-tensor SQUID gradiometer system for geophysical applications," *Leading Edge*, vol. 25, pp. 178–180, doi: 10.1190/1.2172308.

Sui Y, Kang P, Cheng D, Lin J (2015), "Analysis and simulation of flight effects on an airborne magnetic gradient tensor measurement system," *IEEE Trans. Instrum. Meas.*, vol. 64, pp. 2657–2665, doi: 10.1109/TIM.2015.2420377.

Sui Y, Li G, Wang S, Lin J (2014), "Compact fluxgate magnetic full-tensor gradiometer with spherical feedback coil," *Rev. Sci. Instrum.*, vol. 85, 014701, doi: 10.1063/1.4856675.

Sunderland A, Ju L, Blair D G, McRae W, Veryaskin A V (2009), "Optimizing a direct string magnetic gradiometer for geophysical exploration," *Rev. Sci. Instrum.*, vol. 80, 104705, doi: 10.1063/1.3227237.

Tilbrook D L (2009), "Rotating magnetic tensor gradiometry and a superconducting implementation," *Supercond. Sci. Technol.*, vol. 22, 075002, doi: 10.1088/0953-2048/22/7/075002.

Voigt J, Knappe-Grüneberg S, Gutkelch D, Haueisen J, Neuber S, Schnabel A, Burghoff M (2015), "Development of a vector-tensor system to measure the absolute magnetic flux density and its gradient in magnetically shielded rooms," *Rev. Sci. Instrum.*, vol. 86, 055109, doi: 10.1063/1.4921583.

Yin G, Zhang Y, Fan H, Ren G, Li Z, (2015), "One-step calibration of magnetic gradient tensor system with nonlinear least square method," *Sensors Actuat. A: Phys.*, vol. 229, pp. 77–85, doi: 10.1016/j.sna.2015.03.026.